ELECTROHYDRAULIC ACTUATOR CONTROLLER DESIGN APPLIED TO MOVABLE NOZZLES ON SOUNDING ROCKETS BASED ON IDENTIFIED MODEL USING SUBSPACE METHODS

EULER GONÇALVES BARBOSA*, RAPHAELA CARVALHO MACHADO#, CÉSAR MOURA BATAGINI*, LUIZ CARLOS SANDOVAL GÓES#

**DCTA-IAE Aeronautical and Space Institute, Praça Marechal Eduardo Gomes, 50, São José dos Campos, SP, CEP 12228-904*

#DCTA-ITA Technological Institute of Aeronautics, Praça Marechal Eduardo Gomes, 50, São José dos Campos, SP, CEP 12228-904

E-mails: `euleregb@iae.cta.br, raphaelarcm@ita.br, cesarcmb@iae.cta.br, goes@ita.br`

Abstract— This work presents a controller design to an electrohydraulic actuator applied to movable nozzles on microsatellites launchers vehicle and sounding rockets using models obtained from closed loop identification, to improve requirements to step-unit response as rise time (bandwidth) and overshot. The plant identification or dynamic system identification to the Electro hydraulic actuator was obtained preliminarily using subspace methods. The actuator is being developed to TVC system applied to Brazilian nozzles to attitude control, at the Aeronautic Technician Center (DCTA). The design criteria is to obtain rise time lower than 60 mili-seconds and 20 percent of overshot. The open loop transfer functions were identified from tests using simple proportional controllers and the controller designed is performed using the multiple rootlocus approach. The digital controller is implemented and validated using a real-time system. Others control extrategies are discussed using analog and digital controllers to the electrohydraulic actuator. Unit-step response are compared using closed loop data from test for validation.

Keywords— Electrohydraulic actuator, controller design, system identification.

Resumo— Este trabalho apresenta o projeto de u controlador para um atuador eletrohidráulico aplicado a tubeiras moveis em veículos lançadores de microssatélites e veículos de sondagem utilizando modelo obtidos de identificação em malha fechada, para melhorar requisito de resposta ao degrau unitário como tempo de subida (banda passante) e sobressinal. A identificação da planta ou identificação de sistema dinâmico para o atuador eletrohidráulico foi obtida preliminarmente utilizando métodos de subespaço. O atuador esta sendo desenvolvido para o sistema TVC aplicado a tubeiras nacionais para controle de atitude, no Centro Técnico Aeroespacial (DCTA). O critério de projeto é obter tempo de subida menor que 60 ms e 20% de sobressinal. A As funções de transferência de malha aberta foram identificadas de testes utilizando controladores proporcionais e o projeto do controlador é realizado utilizando a abordagem do múltiplo lugar das raízes. O controlador digital é implementado e validado com um sistema de tempo-real. Outras estratégias de controle são discutidas utilizando controladores analógicos e digitais para o atuador eletrohidráulico. A respostas ao degrau unitário são comparadas utilizando dados em malha frechada de dados de testes de validação.

Palavras-chave— Atuador eletro hidráulico, Projeto de controlador, Identificação de sistemas.

1 Introduction

The thrust vector control system applied to attitude control consists of a movable nozzle operated by an electro-hydraulic actuator (EHA) and a flexible joint, as shown in the Figure (1). This system is applied to controlled vehicles, e. g. the Brazilian Microsatellite Launcher Vehicle VLM-1, described in details in (Loures da Costa et al., 2012), and to sounding rockets purposes. Actually new extrategies are being considered concerning the development of new technologies to the EHA to support such vehicles. The EHA is one of them, where the Institute of Aeronautics and Space (IAE) has projects focused on Pressure Fed Systems (PFS) using different hydraulic pressure, new materials, gas, new cylinders, new controllers and electro hydraulic servo valves (EHSV).

The EHA is a device that has an important function in TVCs systems (Cornelisse et al., 1979), and so its complete dynamics behavior must be known in details. The IAE facilities permits the characterizing and to test several types of EHA, presented in the Fig 2. It consists of a workbench with a mass-spring-dump load attached to the rod of the EHA. A real-time system is available to digital control design validation, as well as to open-loop and closed-loop identification.

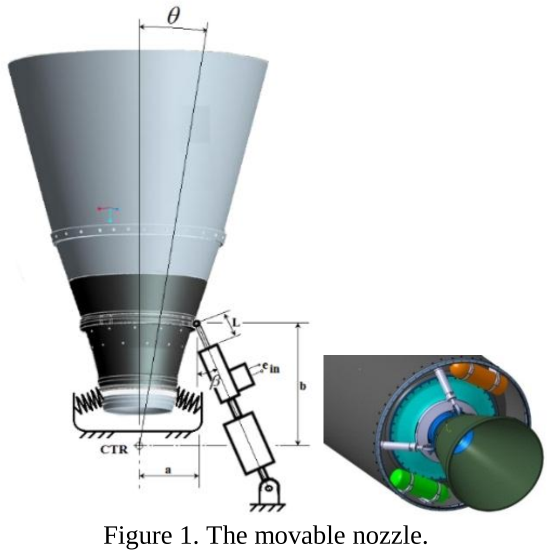

Figure 1. The movable nozzle.

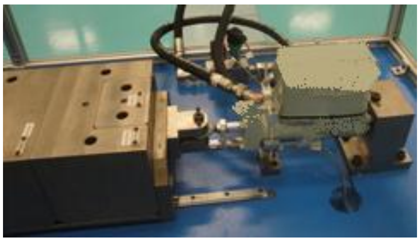

Figure 2.The Electrohydraulic actuator workbench.

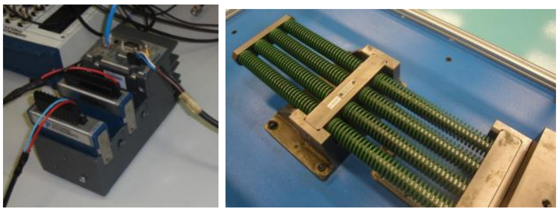

Figure 3. (left) – CompactRIO system and (right) load: springs, mass and damping.

The EHA can operate in open-loop or closed-loop manner detailed in (Merrit, 1991) and (Jelali and Kroll, 2003). In the first case some EHA needs an external feedback because its integration action. In the second case the external feedback can be used to improve dynamic response like time-domain specifications as well as to reduce or eliminate the steady-state error. So it is mandatory the identification of its linear or nonlinear dynamics, to control designs and validation. This work presents the results obtained from PID control design based on models from closed-loop identification using subspace approach and the multiple root-locus technique to control design and validation to a specific EHA.

In (Barbosa et al., 2013) is discussed a nonlinear dynamic behavior to a TVC system using this EHA. The work of (Werkerly et al., 2016a) presents the Status of Brazilian Thrust Vector Control System Development and (Werkerle et al., 2016b) presents the closed-loop actuator identification for Brazilian Thrust Vector Control development.

2 The Plant and Real-Time Controller

The Figure 4 presents the simplified control system to the EHA closed-loop operation. The CompctRIO (CRIO) performs the digital control to the EHA. ADCs and DACs converters are used to generate and to collect data with sample frequency of 100Hz and 200Hz.

The Figure 4 shows the block diagram to the digital EHA control system, while the Figures 5 and 6 present the devices and general blocks for the feedback control

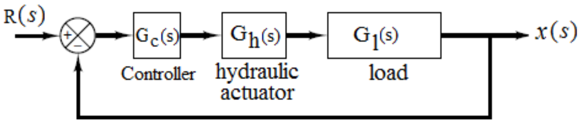

Figure 4. Control system to the EHA operation.

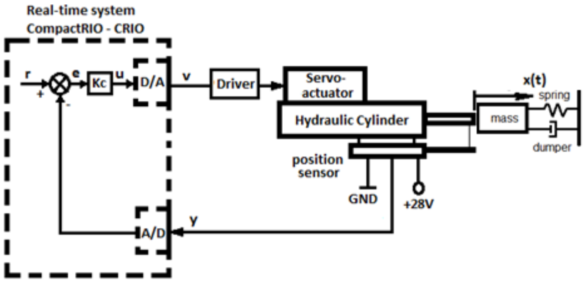

Figure 5. Control system to the EHA operation.

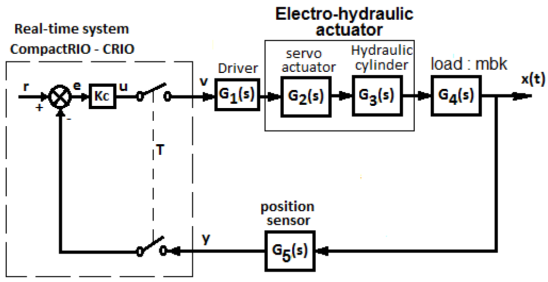

Figure 6. Block diagram to the digital EHA control system.

The Figure 7 presents the digital controller in LabVIEW environment.

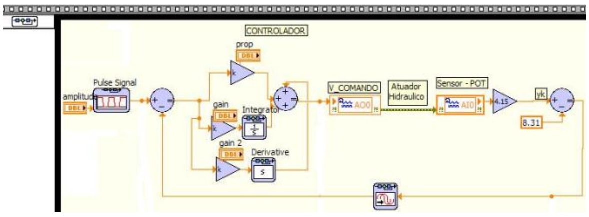

Figure 7. The CRIO PID controller.

3 Plant Identification and Subspace Methods

The identification processes detailed in (Ljung, 1999) and the subspace identification methods refers to an algorithms class of parametric identification where model form is on discrete state space, according to (Katayama, 2005) and (Machado, 2013). SIM methods (subspace identification methods) have a main character recover the system matrix from a vector projection from observed input-output data (Moor et al., 1996). The classical application of identification techniques consists in tests with system operating in open-loop operation and the noise is uncorrelated with input data. In this case, the SIM methods seems work well. However, in some cases it is not possible to identify the system in open-loop, due to its instability behavior (unstable in open-loop, integrator behavior or security condition), the closed-loop identification is necessary.

The main difficulty with closed-loop identification is the correlation with noise and the input data caused by feedback. In this sense, SIM methods seems produce results more favorable than classical methods. In this work the SIM method known as DSR_e (combined deterministic and stochastic system identification and realization), proposed by Ruscio (2008), can be applied in both cases open and closed-loop. The linear model obtained from the subspace method was chosen as a third order, so we have:

$$x_{k+1} = Ax_k + Bu_k + K\varepsilon_k$$
$$y_k = Cx_k + \varepsilon_k$$

which x_k is the system states vector, u_k is the input vector, y_k is the output vector and "k is the innovation method. The identification problem consists in determine the model matrices A,B and C and the Kalman gain K. The matrix D is assumed to be null. The DSR_e algorithm proposed by (Ruscio, 2008) is a SIM method composed of basically two steps. In the first step the experimental data are separed in two components, a signal named yd J=1 and a innovation sequence, "J=1”. In the second step, a state space model is obtained from deterministic identification deterministic, described in (Ruscio, 2008).

The algorithm DSR_e proposed by (Ruscio, 2008) was implemented in (Machado, 2013) and applied for system identification.

In (Machado, 2013) the first step is according to the original version, however opted to use the deterministic subspace algorithm N4SID (numerical algorithms for subspace state space system identification) to solve the determination the order and system matrices. The Figure 8 presents the block diagram of algorithm DSR_e. The identification parameters are the past horizons J and future horizons L used to construct the data matrices.

The SIM method apply LQ factorization (transpose of QR factorization) and SVD decomposition (singular value decomposition), in (Aguirre, 2007), to obtain, respectively, the observability matrix, and model of order n. Then finally, a state sequence estimated, we can obtain the matrices A, B e K solving the LS (least squares) regression problem.

$$x_{k+1} = Ax_k + \begin{bmatrix} B & K \end{bmatrix} \begin{bmatrix} u_k \\ \varepsilon_k \end{bmatrix} \qquad (1)$$
$$y_k^d = Cx_k$$

details about the subspace algorithm equation can be found in (Machado, 2013).

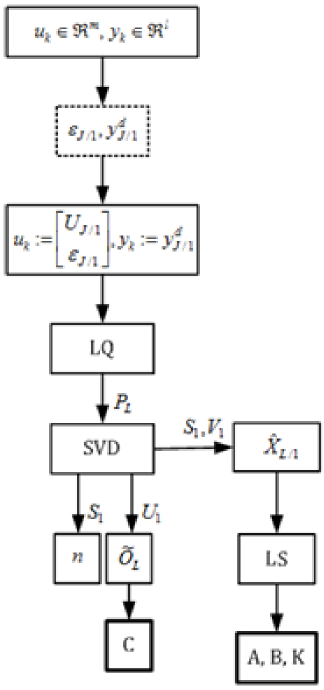

Figure 8. DSRe method (Machado, 2013).

The closed-loop identification using subspace method produced the following third order models using aleatory signal and PRBS signal of excitation:

Signal excitation	MRSE [%]	Identified poles
PRBS	29.84	-22.65, -143.65± j119.85
Aleatory	16.23	-29.07, -131.95±j127.12

Table 1 - Poles from closed-loop identification and MRSE index.

obtaining to the following plant transfer function:

$$G(s) = \frac{e(s^2 + fs + g)}{(s+a)(s^2 + cs + d)} \qquad (2)$$

and numerically:

$$G(s) = \frac{14.91(s^2 - 417.7s + 64700)}{(s + 29.07)(s^2 + 263.9s + 33570)} \qquad (3)$$

so the parameters are

a = 29.05 e = 14.91
c = 263.9 f = -417.7
d = 33570 g = 64700

The model presents a second order dynamic system in which its complex poles are -131.95 ± j127.12 rad/s. The Figure 9 shows the results obtained assigning the first order pole at 30 rad/s, from experimental data and identification processes.

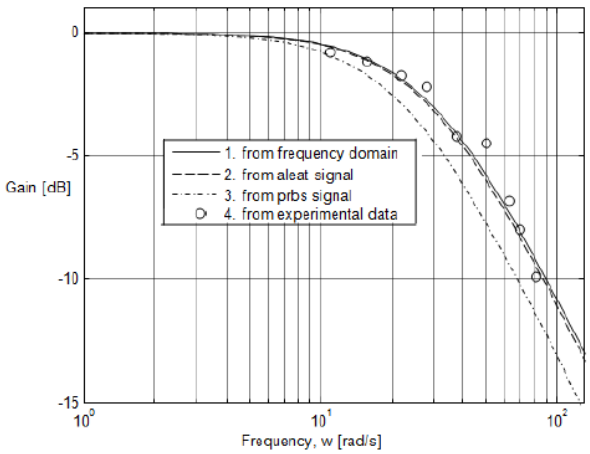

Figure 9: Gain versus frequency, open-loop operation using sine wave excitation, closed-loop operation via aleatory and PRBS signals of excitation.

4 PID design - the multiple root locus approach

The PID controller, described in widely literature as (Aström, 1988), (Ogata, 2010), and (Franklin, 1991), improves the dynamic response as well as to reduce or eliminate the steady-state error. The actually proportional unit-step response is presented in the Figure 10.

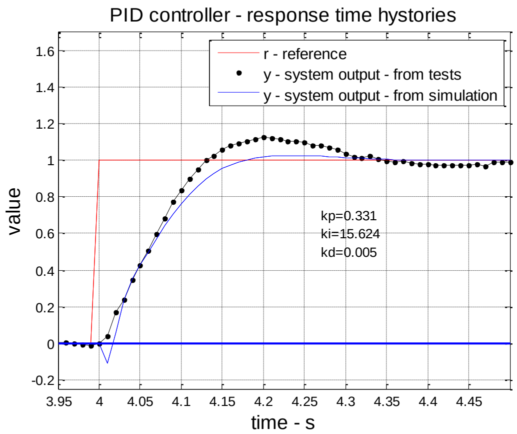

Figure 10. Unit-step time response.

It can be noted that the rise time and overshoot are $t_r = 90ms$ and $M_p > 10\%$ respectively. In this work the design requirements to the closed-loop specifications are:

$t_r < 60ms$	rise time
$M_p < 30\%$	overshoot

The relative location of the poles can be considered and we can apply the dominant second-order closed-loop poles approach to define the limits as follows, just as reference on choosing of PID gains.

i. the overshoot Mp equations produces the damping ratio:

$$M_p = e^{\frac{-\xi\pi}{\sqrt{1-\xi^2}}} \qquad \xi > 0.45$$

ii. And the rise time and damping ratio defines the undamped natural frequency:

$$t_r = \frac{\pi-\beta}{\omega_n\sqrt{1-\xi^2}} \quad \text{and} \quad \beta = \arccos\xi$$

$$\text{so} \quad \omega_n = \frac{\pi - \arccos\xi}{t_r\sqrt{1-\xi^2}} \qquad \omega_n > 50.2 rad/s$$

The multiple root locus approach consists of plotting a set of root locus, performed with parameters of interest. Let the generically characteristic equation due to closed-loop transfer function $T(s), \Delta(s) = 0$ as follows.

$$D(s) + k_1 N_1(s) + k_2 N_2(s) + ... + k_n N_n(s) = 0 \quad (4)$$

As a step 1 we assign: $k_2 = k_3 = ... = k_n = 0$

$$\Delta_1(s) = D(s) + k_1 N_1(s) = 0$$

base root locus:

$$1 + k_1\frac{N_1(s)}{D(s)} = 0 \quad (5)$$

$$k_1 \in [0,\infty); \quad k_2 = k_3 = ... = k_n = 0$$

As a step 2:

$$k_1 = \bar{k}_1; k_2 \in [0,\infty); \quad k_3 = k_4 = ... = k_n = 0$$

$$\Delta_2(s) = D(s) + \bar{k}_1 N_1(s) + k_2 N_2(s) = 0$$

and applying the golden rule:

$$1 + k_2\frac{N_2(s)}{D(s) + \bar{k}_1 N_1(s)} = 0 \quad (6)$$

$$k_2 \in [0,\infty)$$

as a step 3:

$$k_1 = \bar{k}_1; k_2 = \bar{k}_2 \; k_3 \in [0,\infty);$$

$$k_4 = k_5 = ... = k_n = 0$$

and applying the golden rule:

$$1 + k_3\frac{N_3(s)}{D(s) + \bar{k}_1 N_1(s) + \bar{k}_2 N_2(s)} = 0$$

$$1 + k_3\frac{N_3(s)}{\Delta_2(s)} = 0 \quad (7)$$

$$k_3 \in [0,\infty)$$

finally at step n:

$$k_1 = \bar{k}_1; k_2 = \bar{k}_2 \; k_n \in [0,\infty);$$

$$\Delta_n(s) = \Delta_{n-1}(s) + k_n N_n(s) = 0$$

and applying the golden rule:

$$1+k_n\frac{N_n(s)}{\Delta_{n-1}(s)}=0 \qquad (8)$$

$$k_n \in [0,\infty)$$

so, applying the multiple root locus approach to the closed loop transfer function or transmission function *T(s)*:

$$T(s)=\frac{(k_p s+k_i+k_d s^2)e(s^2+fs+g)}{s(s+a)(s^2+cs+d)+(k_p s+k_i+k_d s^2)e(s^2+}$$

with the characteristic equation:

$$\begin{aligned}\Delta(s)=&s(s+a)(s^2+cs+d)+\\&+(k_p s+k_i+k_d s^2)e(s^2+fs+g)\end{aligned} \qquad (9)$$

Rewrited as

$$\begin{aligned}\Delta(s)=&s(s+a)(s^2+cs+d)+\\&+k_p se(s^2+fs+g)+\\&+k_i\, e(s^2+fs+g)+\\&+k_d\, e s^2(s^2+fs+g)\end{aligned}$$

So the polynomials are, according to Eq 6 and 7,

$$\begin{aligned}D(s)&=s(s+a)(s^2+cs+d)\\N_1(s)&=e\,s(s^2+fs+g)\\N_2(s)&=e\,(s^2+fs+g)\\N_3(s)&=e\,s^2(s^2+fs+g)\end{aligned} \qquad (10)$$

the base root locus is defined as

$$1+k_p\frac{e(s^2+fs+g)}{(s+a)(s^2+cs+d)}=0$$

$$k_p\in[0,\infty); \qquad k_i=k_d=0$$

the base root locus is presented in the Figure 11 as follows.

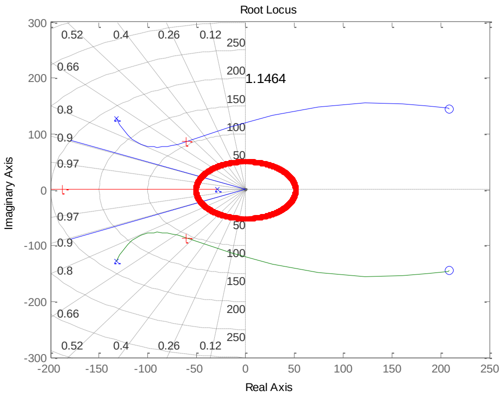

Figure 11. Base root locus

The pole related to the sampling frequency, 200Hz (T=5ms), is:

$$p_s=-\frac{2}{T}=-\frac{2}{0.005}=-400 \text{ rad/s}$$

In which is assumed with no influence on PID control design. The first multiple root-locus is obtained from Eq. (6):

$$1+k_i\frac{e(s^2+fs+g)}{s(s+a)(s^2+cs+d)+\bar{k}_p e\,s\,(s^2+fs+g)}=0$$

with:

$$k_p=\bar{k}_p \qquad k_i\in[0,\infty) \qquad k_d=0$$

The Figure 12 shows the first multiple root locus.

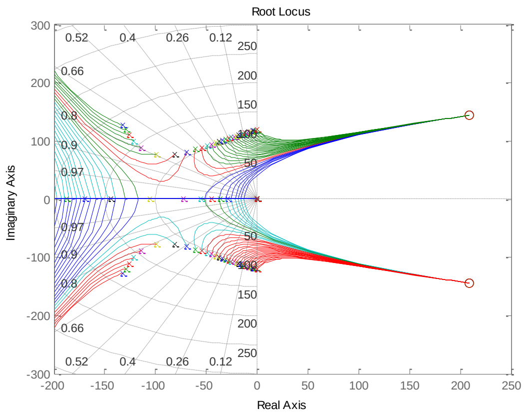

Figure 12. First multiple root locus.

The polynomials to the second multiple root-locus are

$$1+k_d\frac{e\,s^2(s^2+fs+g)}{\begin{aligned}s(s+a)(s^2+cs+d)+\bar{k}_p e\,s\,(s^2+fs+g)+\\+\bar{k}_i e\,(s^2+fs+g)\end{aligned}}=0$$

with:

$$k_p = \bar{k}_p \qquad k_i = \bar{k}_i \qquad k_d \in [0, \infty)$$

the *second multiple root locus* is obtained with $k_p \in [0, \infty)$, $k_i = \bar{k}_i$ and $k_d = \bar{k}_d$, shown in Fig. 7.

The Figures 13 and 14 shows the first multiple root locus.

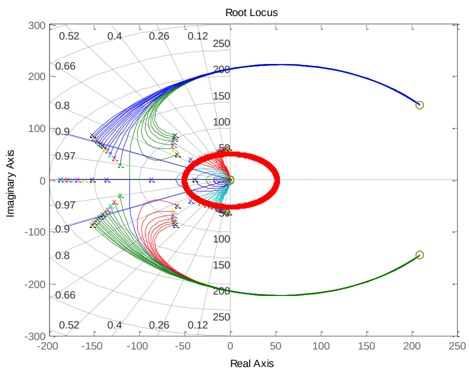

Figure 13. Second multiple root locus

The Figure 14 shows the final root locus where are pointed out the closed loop poles obtained using the PID controller.

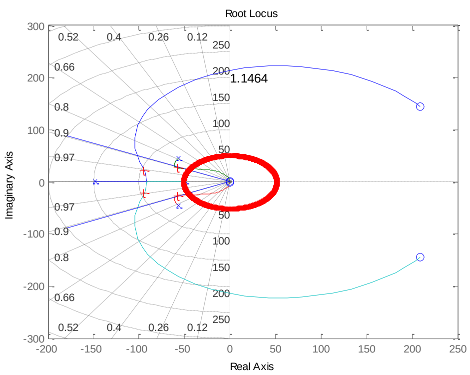

Figure 14. Final system root-locus.

5 Results and closed-loop time performance

The figures as follow show the unit-response of the closed-loop control using the PID gains calculated in the previous section. The Fig. 15 shows the results using kp=0.251, ki=15.624 and kd=0.005.

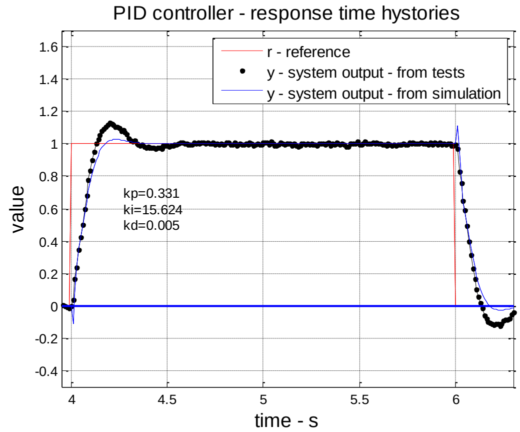

Figure 15. Unit-step time response.

The Figure 16 shows an amplification of figure 14 (zoom) and we can note the rise time and overshot obtained with the PID gains.

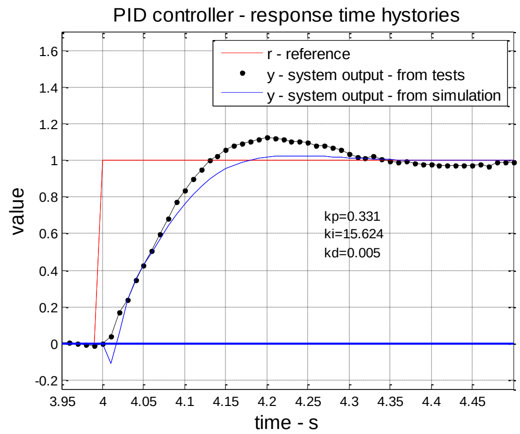

Figure 16. Unit-step time response (zoom).

The undershots on the unit-step response, shown in Fig. (16) and (18) are is due to *zeros* on plant model identified in closed loop operation using subspace methods.

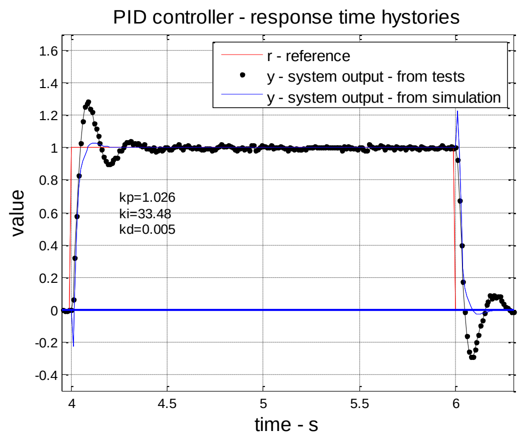

Figure 17. Unit-step time response.

The Figure 18 shows an amplification of figure 16 (zoom) and we can note the rise time and overshot obtained with the PID gains.

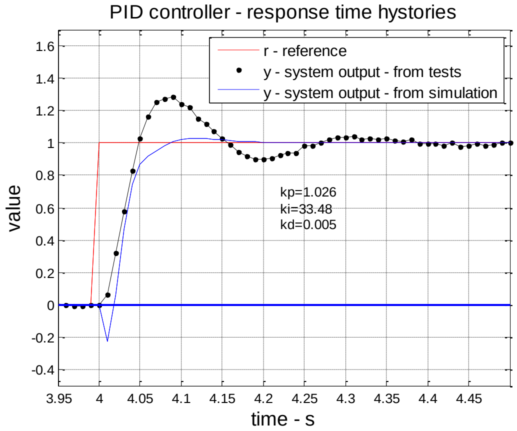

Figure 18. Unit-step time response (Zoom).

The performance criteria used to characterize the transient response to a unit-step input include rise time, peak time, overshot Mp and settling time. The rise time t_r is the time required for the response to rise from 10 percent of the final value to 90 percent of the final value.

Graphical results shows the following time specifications. The rise time of 35ms and overshot 28% was obtained, attending the preliminary control requirements:

Set #1:

(PID, closed-loop identified model, 200Hz, kp = 0.331, ki = 15.624, kd = 0.005)

t_r = 100ms Mp = 3% (simulated)

t_r = 95ms Mp = 12% (from tests)

Set #2:

(PID, closed-loop identified model, 200Hz, kp=1.026, ki = 33.480, kd = 0.005)

t_r = 40ms Mp = 3% (simulated)

t_r = 35ms Mp = 28% (from tests)

6 Conclusions

The main conclusion of this work is that the closed loop EHA design presented performance according to EHAs applied to TVCs systems. The success on PID design using identified model from subspace approach was discussed in details, as well as the design toll known as multiple root-locus technique. The PID controller was validated using a real-time platform.

The PID controller and the EHA presented a rise time and overshot of 35ms and 28% respectively, attending the preliminary design requirements. Some results from simulations presented undershot due to zeros in the identified plant.

This work is a guideline for next controllers design applied to Brazilian EHA projects, as well as to electro hydraulic servo-valve preliminary projects.

The closed-loop model identification is the solution to some EHA identification just because the integrator characteristic of such devices in open-loop operation.

The multiple root locus associated to the golden rule can be applied, with good results, to the PID design control and it can be verified that the closed loop poles stays at the LHP (s-Laplace domain), just collecting the multiple root locus in an interesting direct and ordered manner. The multiple root locus permits to observe the tendency of poles migration through the root locus and so to choose the limits on its parameters.

This approach considers only simplified linear model and any nonlinearity effect must be verified with nonlinear techniques analysis.

Acknowledgments

The authors acknowledge the financial support of SIA Project and technical support of Rafael Ocariz.

References

Aström, K.J., (1988). *Automatic Tuning of PID Controllers*, Instrument Society of America (ISA).

Aguirre, L.A., 2007. Introdução à identificação de sistemas: técnicas lineares e não-lineares aplicadas a sistemas reais. Editora UFMG, Belo Horizonte, Minas Gerais.

Barbosa, Euler G.; Machado, R. C. ; Filho, W., Dynamic Analysis and Identification Of The Movable Nozzle Used On The Brazilian Satellite Launcher. In: COBEM - International Congress of Mechanical Engineering, 2013, Ribeirão Preto.

Cornelisse, J.W., Schoyer, H.F.R., Wakker, K.F. (1979). *Rocket Propulsion and Spaceflight Dynamics*, Pitman Publishig.

Franklin, G. F.; Powell, J. D.; Emami-Naeini, A. (1991) *Feedback control of dynamic systems*. New York, NY.: Addison Wesley Publishing Company.

Merrit, H. E., Hydraulic Control Systems, First Edition, Publisher: Wiley; 1st edition (January 1, 1991), ISBN-10: 0471596175, ISBN-13: 978-0471596172.

Jelali, M., Kroll, A., Hydraulic Servo-systems Modelling, Identification and control - Advances in Industrial Control, Springer; 2003 edition (January 17, 2003), ISBN-13: 978-1852336929.

Katayama, T., 2005. Subspace methods for system identification. Springer, Kyoto, Japan.

Ljung, L., System Identification: Theory for the User, 2nd Edition, Prentice Hall, 1999.

Loures da Costa, L. E., Fulindi, J. B., Di Iorio Jeronymo, A. C. Matos de Carvalho T. H., Ettl, J. "The VLM-1 Launch System Concept," IAC-12-D2.7.10, 63rd International Astronautical Congress, Napolis, Italy, October 1-5, 2012.

Machado, Raphaela C., System Identification using subspace methods, 2013, ITA - Aeronautic Technologic Institute, Brazil, Master degree thesis.

Moor, B.D. and Overschee, P.V., 1996. Subspace identification for linear systems: theory, implementations, applications. Kluwer Academic Publishers, Leuven, Belgium.

Ruscio, D.D., 2008. "Subspace system identification of the kalman filter: open and closed loop systems." In Proc. Intl. Multi-Conf. on Engineering and Technological Innovation.

Verhaegen, M. and Deprettere, E., 1991. "A fast, recursive MIMO state space model identification algorithm". In Decision and Control, 1991., Proceedings of the 30th IEEE Conference on. Vol. 2, pp. 1349–1354.

Wekerle, T.; Barbosa, Euler G. ; Costa, L. E. V. L. ; Trabasso, L. G. . Status of Brazilian Thrust Vector Control System Development. AIAA American Institute of Aeronautics and Astronautics, AIAA Propulsion and Energy Forum and Exposition, 23-25nd July-2016.

Wekerle, T.; Barbosa, Euler G.; Batagini, C. M. ; Costa, L. E. V. L.; Trabasso, L. G. . Closed-loop actuator identification for Brazilian Thrust Vector Control development. IFAC, 20th IFAC Symposium on Automatic Control in Aerospace, ACA 2016, Sherbrooke, Quebec, Canada, 21-25th August-2016.